Directionality of Hydrogen Bonds to Sulfur and Oxygen

J. A. Platts, S. T. Howard,* and B. R. F. Bracke

Contribution from the Department of Chemistry, University of Wales, Cardiff, P.O. Box 912, Cardiff CF1 3TB, U.K.

Received August 21, 1995. Revised Manuscript Received November 6, 1995[⊗]

Abstract: Hydrogen-bonded complexes involving sulfur bases are found to be quite different from the analogous oxygen complexes, both experimentally and in theoretical calculations. In general, hydrogen bonds to sulfur not only are weaker than those to oxygen but also show a marked preference for a more "perpendicular" direction of approach to the donor atom. *Ab initio* calculations at the MP2/6-311++G(d,p) level on the complexes of hydrogen fluoride with H_2O, H_2S, H_2CO, and H_2CS reproduce these differences, as does a search of structures in the Cambridge Crystallographic Data Base. We show that the Laplacian of the charge density $\nabla^2\rho$ predicts a qualitatively correct structure for all the systems considered, but gives poor quantitative predictions of hydrogen-bonding geometries. An analysis based upon Bader's atoms-in-molecules theory rationalizes the differences between sulfur and oxygen hydrogen bonds. A treatment of the hydrogen bond which explicitly considers the contributions of atomic multipoles to the electrostatic energy has more success than $\nabla^2\rho$ in predicting H bond directionality. Hydrogen bond formation to oxygen is driven by charge−charge interactions, whereas with sulfur the stabilization arises principally from the interaction of the charge on the acidic hydrogen with the dipole and quadrupoles of sulfur.

Introduction

Ab initio calculations on hydrogen-bonded systems are becoming increasingly common in the literature,[1] and with advances in computational power such calculations yield ever better agreement with experiment. For small systems, large polarized and diffuse basis sets have become almost *de rigeur*, while electron correlation is clearly essential for useful quantitative predictions of H bond energies. Most calculations on hydrogen-bonded complexes employ the supermolecule approach, whereby the H bond strength is taken to be the energy of the complex minus the energy of the constituent monomers. Though this raises the problem of basis set superposition error (BSSE), this method is generally favored over those which attempt to describe the hydrogen bond purely from the properties of the monomers.

Also common are attempts to obtain further information on the nature and origin of hydrogen bonds. The seminal work of Buckingham and Fowler[2] showed that the electrostatic properties of monomers are sufficient to predict hydrogen-bonding geometries (and to some extent the binding energies) of small first- and second-row molecules with reasonable accuracy. In a similar vein, Carroll *et al.*[3] showed the Laplacian of the charge density $\nabla^2\rho$, a function which neatly characterizes lone pair (LP) positions, also gives reasonable predictions of the structures of a wide range of BASE···H−F complexes. The application of Bader's atoms-in-molecules (AIMs) decomposition technique,[4] which divides the continuous electron distribution into nonoverlapping atomic basins, provides a route for elucidating the nature of H bonds via atomic multipoles and energies and their changes on complexation.[3,5,6]

Most reported calculations on hydrogen bonds have considered only complexes containing first-row atoms. Studies of second-row complexes, although less common, are numerous enough for trends down groups to be observed. One well-known trend is that hydrogen bonds become weaker descending down a given group,[7] usually rationalized on the basis of relative electronegativities. Another less-noted trend is the preference of sulfur to form hydrogen bonds with more "perpendicular" angles than oxygen (see Figure 1), an effect which is limited to group VI atoms. This observation comes mainly from theoretical calculations, but is reinforced by both gas phase spectroscopic[8] and crystallographic measurements, as we will demonstrate. It has been suggested that this results from different hybridization of the valence orbitals in oxygen and sulfur.[7] A more rigorous argument is based on electrostatics: within most definitions of atomic charge (divalent) sulfur atoms are usually positive and oxygens negative, so it is clear that the nature of hydrogen bonds involving these atoms could be fundamentally different.

Local maxima in $-\nabla^2\rho$, so-called (3, −3) critical points (CPs), are found in the expected positions of the lone pairs (LPs) in Lewis theory, and also in bonds involving heavy atoms (identified with bonding pairs, BPs). The theory of reactivity based on $\nabla^2\rho$ considers alignment of acceptors (with electron-deficient regions) and electron-rich donors[4b,9] (e.g., oxygen/sulfur LP regions in this case). Carroll *et al.*[3] utilized these LP local maxima to predict H-bonding directions with some success. This approach seemed promising for rationalizing the sulfur/oxygen differences considered in this work. However, we will

[⊗] Abstract published in *Advance ACS Abstracts,* March 1, 1996.

(1) See for example: (a) Frisch, M. J.; Pople, J. A.; DelBene, J. E. *J. Phys. Chem.* **1985**, *89*, 3664 and references cited therein. (b) Frisch, M. J.; DelBene, J. E.; Binkley, J. S.; Schaefer, H. F., III. *J. Chem. Phys.* **1986**, *84*, 2279. (c) Schaefer, H. F., III; Yamaguchi, Y. *J. Mol. Struct. (THEOCHEM)* **1986**, *135*, 369. (d) Delbene, J. E. *J. Chem. Phys.* **1987**, *86*, 2110. (e) Latajka, Z.; Scheiner, S. *Chem. Phys.* **1988**, *122*, 413. (f) Kim, K. S.; Mhin, B. J.; Choi, U. S.; Lee, K. *J. Chem. Phys.* **1992**, *97*, 6649. (g) Bacskay, G. B. *Mol. Phys.* **1992**, *77*, 61. (h) Saebo, S.; Tong, W.; Pulay, P. *J. Chem. Phys.* **1993**, *98*, 2170. (i) Dobado, J. A.; Molina, J. M. *J. Phys. Chem.* **1993**, *97*, 11415.

(2) Buckingham, A. D.; Fowler, P. W. *Can. J. Chem.* **1985**, *63*, 2018.

(3) Carroll, M. T.; Bader, R. F. W. *Mol. Phys.* **1988**, *63*, 387.

(4) (a) Bader, R. F. W.; Nguyen-Dang, T. T. *Adv. Quantum Chem.* **1981**, *14*, 63. (b) Bader, R. F. W. *Atoms in Molecules: A Quantum Theory;* Oxford University Press: Oxford, 1990. (c) Bader, R. F. W. *Chem. Rev.* **1991**, *91*, 893.

(5) Carroll, M. T.; Bader, R. F. W. *Mol. Phys.* **1988**, *65*, 695.

(6) Platts, J. A.; Laidig, K. E. *J. Phys. Chem.* **1995**, *99*, 6487.

(7) Sennikov, P. G. *J. Phys. Chem.* **1994**, *98*, 4973, and references cited therein.

(8) Legon, A. C.; Millen, D. J. *J. Am. Chem. Soc.* **1987**, *109*, 356.

(9) Bader, R. F. W.; MacDougall, P. J.; Lau, C. D. H. *J. Am. Chem. Soc.* **1984**, *106*, 1594.

0002-7863/96/1518-2726$12.00/0

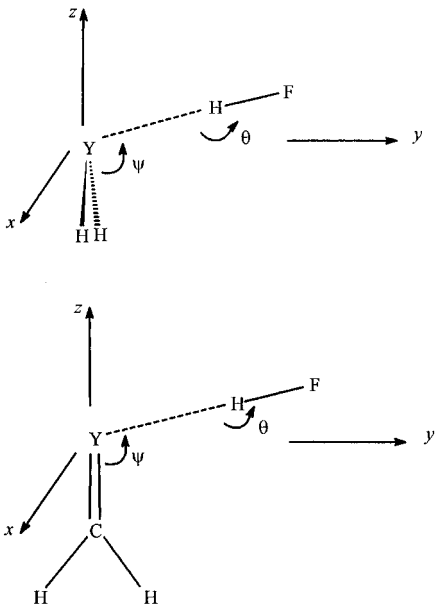

Figure 1. Orientation of H-bonded complexes and the coordinate frame employed.

show that when a consistently high level of theory is applied to two sulfur- and two oxygen-containing BASE−HF complexes, H-bonding directions based on $-\nabla^2\rho$ LP maxima are poor in two of the four cases (one sulfur and one oxygen).

As the starting point for studying these hydrogen bonds, we have carried out high-level geometry optimizations on the complexes of HF with H_2O, H_2S, H_2CO, and H_2CS, and the corresponding monomers. Furthermore, we have applied Bader's AIMs decomposition to the charge distributions. This enabled us not only to analyze the changes in atomic populations, energies, *etc.* as have Carroll *et al.*[3] but also to estimate the electrostatic binding energy between base and acid. This is done in the manner of Buckingham and Fowler,[2] expanding the electrostatic potential energy in terms of atom-centered multipole moments. Our treatment differs from theirs, however, in that (i) we use multipole moments obtained from the AIMs decomposition rather than "distributed Multipoles"[10] and (ii) we fix the S···H and O···H distances at those found from the *ab initio* optimization, instead of the sum of the van der Waals radii.

Computation

All geometry optimizations have been performed at the MP2(FC)/6-311++G(d,p) level of theory[11,12] using the GAUSSIAN92 package[13] supported on the University of London's Convex C3800 supercomputer. For the base molecules C_{2v} symmetry was employed, while the BASE···H−F complexes were optimized with C_s symmetry. The complex geometries are illustrated schematically in Figure 1. Subsequent analysis of the charge distributions and wave functions used the same treatment of correlation and basis set in order to avoid nonzero Hellman−Feynman forces making unknown contributions to the calculated properties.[4] Checks were made to ensure that atomic properties sum to the correct molecular value. Corrections for BSSE to the H bond energies were made using the counterpoise method due to Boys and Bernardi.[14]

In the case of complexes of the type $R_2C{=}Y\cdots HX$ (analogous to our $H_2CO\cdots HF$ and $H_2CS\cdots HF$ complexes) a statistical analysis of such intermolecular contacts in the Cambridge Structural Database[15] revealed an angular distribution of hydrogen bonds with a well-defined maximum. Searching employed appropriate constraints on the geometry and accuracy of the structures to ensure only suitable hydrogen-bonded contacts were selected: 5419 suitable crystal structures were found for oxygen-containing bases, and 442 for the sulfur complexes. Similar attempts to analyze the geometry of intermolecular contacts of the type $R-O-R'\cdots HX$ and $R-S-R'\cdots HX$ yielded no apparent preference for the H-bonding angle ψ (see Figure 1). This is presumably because other effects of crystal packing (the presence of other interactions, bulky groups, *etc.*) rather determine the relative orientation of the moieties when the oxygen or sulfur atom is less sterically accessible for hydrogen bonding (in contrast to −C═O and −C═S groups). We therefore do not report any results for these searches.

Having optimized the geometries of all the systems considered, we carried out topological analysis of the distributions $\rho(\mathbf{r})$ and $\nabla^2\rho(\mathbf{r})$ following the method of Bader.[16,17] CPs in $\rho(\mathbf{r})$ are identified with nuclei, bonds, rings, and cages according to the curvatures of the density at the critical point. Of interest here are the (3, −1) or bond CPs in $\rho(\mathbf{r})$, invariably found between two interacting atoms. Critical points in $-\nabla^2\rho(\mathbf{r})$ can be similarly characterized, the most relevant here the local maxima or (3, −3) CPs, which have been shown to reproduce the expected behavior of Lewis electron pairs.[4b,9] The topological analysis of the charge distribution employed the AIMPAC suite of programs,[16] in particular the programs EXTREME and BUFFALO. We will use the subscript c to denote properties computed at a bond CP, e.g., ρ_c and $\nabla^2\rho_c$.

Integrated atomic properties were calculated using the AIMPAC program PROAIMV. The boundaries of an atomic subsystem (Ω) are defined so that the subsystem obeys the "zero-flux" condition, *i.e.*

$$\nabla\rho(\mathbf{r})\cdot\mathbf{n}(\mathbf{r}) = 0$$

for all points **r** on the surface (**n** is a vector normal to this surface). Subsystems so defined obey the virial theorem.[4b,18] An atomic property density, $\rho_A(\mathbf{r})$, corresponding to an observable $\hat{A}$ is integrated over all space to yield the expectation value of $\hat{A}$ for the total system. Similarly, atomic expectation values are found by integration over the atomic basin Ω, defined by the zero-flux condition, *i.e.*

$$A(\Omega) = \int_\Omega d\tau\, \rho_A(\mathbf{r})$$

In this manner, atomic properties such as populations and charges,[19] total energies,[3,20] volumes,[21] and multipole moments[22] can be determined.

The base MEP and complex electrostatic interaction energies have been calculated from the AIMs multipole moments up to the quadrupole level, using well-known formulas[23] incorporated in an in-house

(10) Stone, A. J. *Chem. Phys. Lett.* **1981**, *83*, 233. *J. Am. Chem. Soc.* **1984**, *106*, 1594.
(11) Moller, C.; Plesset, M. S. *Phys. Rev.* **1934**, *46*, 618.
(12) (a) Krishnan, R.; Binkley, J. S.; Pople, J. A. *J. Chem. Phys.* **1980**, *72*, 650. (b) Hariharan, P. C.; Pople, J. A. *Theor. Chim. Acta* **1973**, *28*, 213. (c) Frisch, M. J.; Pople, J. A.; Binkley, J. S. *J. Chem. Phys.* **1984**, *80*, 3265.
(13) Frisch, M. J.; Trucks, G. W.; Head-Gordon, M.; Gill, P. M. W.; Wong, M. W.; Foresman, J. B.; Gonzalez, C.; Martin, R. L.; Fox, D. J.; Defrees, D. J.; Baker, J.; Stewart, J. J. P.; Pople, J. A. *Gaussian 92, Revision B;* Gaussian, Inc.: Pittsburgh, PA, 1992.
(14) Boys, S. F.; Bernardi, F. *Mol. Phys.* **1970**, *19*, 553.
(15) Allen, F. H.; Davies, J. E.; Galloy, J. J.; Johnson, O.; Kennard, O.; MacRae, C. F.; Mitchell, E. M.; Mitchell, G. F.; Smith, J. M.; Watson, D. G. *J. Chem. Inf. Comput. Sci.* **1991**, *31*, 187.
(16) Biegler-König, F. W.; Bader, R. F. W.; Tang, T. H. *J. Comput. Chem.* **1982**, *3*, 317.
(17) Bader, R. F. W.; Essen, H. *J. Chem. Phys.* **1984**, *56*, 1943.
(18) Srebrenik, S.; Bader, R. F. W. *J. Chem. Phys.* **1975**, *63*, 3945.
(19) (a) Bader, R. F. W.; Cheeseman, J. R.; Laidig, K. E.; Wiberg, K. B.; Breneman, C. *J. Am. Chem. Soc.* **1990**, *112*, 6530.(b) Bader, R. F. W.; Zou, P. F. *Chem. Phys. Lett.* **1992**, *91*, 54. (c) Glaser, R.; Choy, G. S.-C. *J. Am. Chem. Soc.* **1993**, *115*, 2340.
(20) Bader, R. F. W.; Chang, C. *J. Phys. Chem.* **1989**, *93*, 5095.
(21) Bader, R. F. W.; Carroll, M. T.; Cheeseman, J. R.; Chang, C. *J. Am. Chem. Soc.* **1989**, *109*, 7968.
(22) (a) Bader, R. F. W.; Larouche, A.; Gatti, C.; Carroll, M. T.; MacDougall, P. J.; Wiberg, K. B. *J. Chem. Phys.* **1987**, *87*, 1142. (b) Laidig, K. E. *Chem. Phys. Lett.* **1994**, *225*, 285. (c) Laidig, K. E. *J. Phys. Chem.* **1993**, *97*, 12760.
(23) (a) Moss, G.; Feil, D. *Acta Crystallogr.* **1981**, *A37*, Appendix C. (b) Jackson, J. D. *Classical Electrodynamics;* John Wiley and Sons: New York, 1962.

Table 1. MP2/6-311++G(d,p) Optimized Monomer Geometries and Optimized Complex Geometries (Å and deg)

(a) Monomer Geometries

	H_2O	H_2S	H_2CO	H_2CS	HF
H−Y[a]	0.960	1.334			
C−Y			1.213	1.614	
H−C			1.105	1.091	
H−Y−H	103.5	92.1			
H−C−Y			121.9	121.9	
H−F					0.917

(b) Optimized Complex Geometries

	$H_2O\cdots HF$	$H_2S\cdots HF$	$H_2CO\cdots HF$	$H_2CS\cdots HF$
H−Y	0.961	1.334		
C−Y			1.218	1.616
H−C			1.100	1.090
H−Y−H	104.7	92.7		
H−C−H			117.3	116.7
H_a−Y[b]	1.731	2.320	1.755	2.221
H_a−F	0.932	0.926	0.931	0.930
ψ[c]	140.1	111.6	114.4	91.2
θ[d]	177.8	179.6	169.5	167.7

[a] Y is the base atom, O or S. [b] H_a is the acidic hydrogen. [c] In complexes of the type H_2 Y···HF, ψ is the hydrogen-bonding angle between the molecular plane of the base and the Y···H vector; in complexes of the type $H_2CY\cdots HF$, ψ is the C−Y···H angle. [d] θ is the angle Y···H−F.

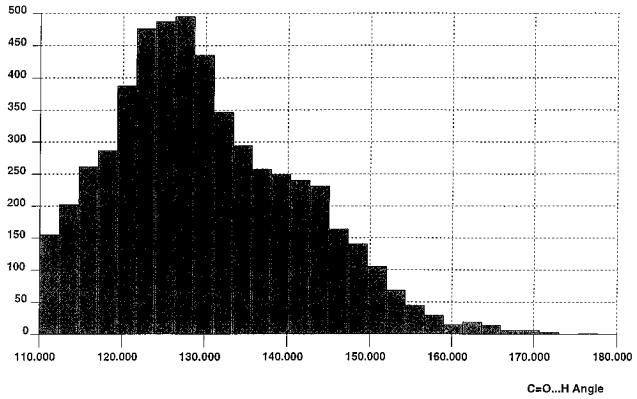

Figure 2. Frequency of database "hits" versus ψ in $R_2CO\cdots HX$.

FORTRAN77 program. To examine the likely convergence of these multipole sums, the base MEP was also evaluated at several points on the C_2 axis, starting at the calculated hydrogen bond distance and taking steps of 0.5 Å away from the base. The multipole expanded MEP at these points has been compared to the "exact" result computed directly from the correlated wave function. In addition, the intermolecular electrostatic interaction energy was calculated from the monomer atomic multipoles at a series of orientations ranging from $\psi = 180°$ to less than 90° (see Figure 1), keeping the Y···H distance fixed at the values found in the *ab initio* calculations. In this treatment, it has been assumed that Y···H−F is colinear ($\theta = 180°$).

Results and Discussion

I. Geometries and Energetics. The results of the MP2-(FC)/6-311++G(d,p) optimizations on HF and on the bases H_2O, H_2S, H_2CO, and H_2CS are reported in Table 1a, and the corresponding results for the BASE−HF complexes in Table 1b. The H bonds to sulfur are around 0.5 Å longer than the analogous bonds to oxygen, as could be expected on the basis of van der Waals radii and relative electronegativities. The H-bonding angles ψ defined in Figure 1 are around 20° smaller in the sulfur complexes than in the corresponding oxygen complexes. These differences also occur in the crystallographic results for $H_2C{=}Y\cdots HX$ type complexes (see Figures 2 and 3), which find mean O···H and S···H distances to be 2.053(4) and 2.620(10) Å, respectively, and mean ψ for O and S complexes to be 130.2(2)° and 108.0(6)°, respectively. The lack of good quantitative agreement between *ab initio* and mean crystallographic hydrogen-bonding angles and distances is to be expected given the diversity of complexes considered in the latter, which often have much bulkier substituents on both base and acid than the hydrogens in our *ab initio* calculations. The importance of these solid state-derived results lies in their support of the trends observed in Table 1b.

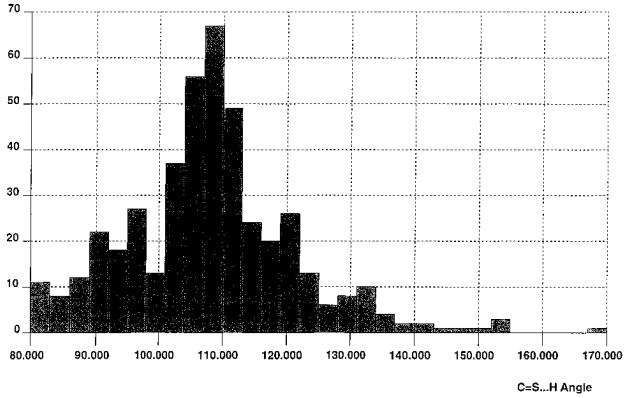

Figure 3. Frequency of database hits versus ψ in $R_2CS\cdots HX$.

Table 2. MP2/6-311++G(d,p) Hydrogen Bond Strengths (kJ·mol^{-1})

	uncorrected H bond energy	counterpoise correction	corrected H bond energy
H_2O	40.2	7.8	32.3
H_2S	22.7	6.9	15.8
H_2CO	32.3	4.7	27.6
H_2CS	26.5	7.3	19.2

Table 3. Relative Energies of Complexes at Equilibrium and with H−F at ±1° (kJ·mol^{-1})

	equilibrium plus 1°	equilibrium	equilibrium minus 1°
H_2O	+0.002	0.0	+0.004
H_2S	+0.010	0.0	+0.076
H_2CO	+0.012	0.0	+0.050
H_2CS	+0.015	0.0	+0.014

H bond energies with and without counterpoise corrections are reported in Table 2. As expected, complexes involving oxygen are more stable than those with sulfur, as found in previous comparative studies on first- and second-row hydrogen bonding.[7] The counterpoise corrections are sizeable (between 4 and 8 kJ·mol^{-1})—almost one-third of the uncorrected H bond energy in one case, but the size of the correction is similar for all complexes, so the stability trend noted above is not affected. Zero-point energy (ZPE) corrections to the interaction energies on formation of the complex would be desirable, but the necessary analytic MP2 harmonic frequency calculations proved to be too computationally demanding.

In this study, the ease of deformation of the H-bonding angle ψ is of central importance. The result that sulfur hydrogen bonds in a more perpendicular fashion than oxygen would be less significant if the force constant corresponding to $\partial^2E/\partial\psi^2$ were much lower in the sulfur complexes. In the absence of analytic harmonic frequencies, we carried out single point energy calculations for each complex with HF displaced ±1° from its optimum angle. These results, given in Table 3, confirm that the optimized geometries are minima with respect to this bending motion, and that complexes containing sulfur are at least as "stiff" with respect to deformations of ψ as their oxygen

Table 4. Selected Bond Critical Point Properties[a] (au)

	ρ	$\nabla^2\rho$	ϵ	r_1	r_2
		H−F			
H−F	0.370	−2.836	0.0000	0.281	1.451
		$H_2O\cdots HF$			
O−H_a	0.037	+0.141	0.064	2.214	1.058
H_a−F	0.347	−2.653	0.000	0.277	1.484
		$H_2S\cdots HF$			
S−H_a	0.020	+0.053	0.027	3.049	1.336
H_a−F	0.357	−2.713	0.000	0.280	1.470
		$H_2CO\cdots HF$			
O−H_a	0.036	+0.130	0.014	2.235	1.084
H_a−F	0.348	−2.644	0.000	2.780	1.482
		$H_2CS\cdots HF$			
S−H_a	0.026	+0.059	0.019	2.927	1.270
H_a−F	0.350	−2.630	0.000	0.281	1.476

[a] ρ is the value of the charge density at the critical point, $\nabla^2\rho$ is the second derivative of the charge density here, ϵ is the ellipticity of the bond, defined as $1 - \lambda_1/\lambda_2$ (the ratio of the two negative curvatures of the charge density), and r_1 and r_2 are the distances from the critical point to A and B in the bond A−B.

counterparts, which explains why the predicted geometrical differences are reflected in experimental studies.

In the course of optimizing these complexes, some interesting (though less important) points came to light. Initial HF/6-311++G(d,p) optimizations resulted in an unrealistic equilibrium geometry of $H_2O\cdots HF$, with HF almost collinear with the C_2 axis of H_2O. Thus, it appears that the reasonable agreement with experiment found with a smaller basis[1a,3] is fortuitous. Including electron correlation effects *via* MP2 theory markedly improves the optimized geometry; we therefore only report the geometries for the MP2/6-311++G(d,p) optimizations. Another feature to be noted in the geometrical data is the angle θ, which measures the nonlinearity of the H bond. In the $H_2CY\cdots HF$ complexes θ is more than 10°, which may be attributed to a secondary attraction of the fluorine with the hydrogen of H_2-CY. However, this value of θ is far less than the 41.5° found for $H_2CS\cdots HF$ by Carroll *et al.* at the HF/6-31G(d,p) level.[3] In fact we find that the structure, as characterized by its charge distribution, differs qualitatively from that reported previously. The use of a larger basis set and the inclusion of correlation (crucial in such weakly bound systems) ensure that these results are more reliable than those in ref 3.

II. Topological Analysis. The topology of ρ proves to be a powerful probe of atomic interactions,[17] and provides a rigorous method for the classification of molecular structure,[24] including hydrogen bonds.[3] Table 4 contains the properties of the charge density at the H bond CPs, and additionally the same data for the H_a−F bonds. The H bonds have properties typical of ionic or closed-shell interactions—low ρ_c and positive $\nabla^2\rho_c$—whereas the H_a−F bonds have features typical of a covalent interaction. The trend of increasing ρ_c and $\nabla^2\rho_c$ in the H bond with increasing H bond strength, which was first noted by Carroll and Bader,[3] is supported by these (more accurate) calculations. A relationship is also evident between the depletion of ρ_c in the H−F bond on complexation and the H bond strength. Bonds within the base fragments show no surprises, being typically covalent and hardly changing their properties on H bond formation, and are therefore not included.

The bond CP analysis highlights an important structural feature in the $H_2CS\cdots HF$ complex. As mentioned above, we find this system to have a structure qualitatively different from that reported by Carroll *et al.*,[3] who found a second intermolecular H-bonding interaction (with an associated bond CP) between the fluorine of HF and the adjacent hydrogen in H_2-CS. This resulted in a very bent H bond and a short H···F contact, and for this reason they did not include this complex in their subsequent study. At the higher level of theory used here, the H···F contact is almost 1 Å longer and there is no sign of a secondary hydrogen bond CP, despite an exhaustive search of the charge density in this region. Their structure was apparently an artifact of the HF/6-31G(d,p) level of calculation.

(24) Bader, R. F. W.; Nguyen-Dang, T. T.; Tal, Y. *Rep. Prog. Phys.* **1981**, *44*, 893.

Table 5. Lone Pair (3, −3) Critical Points in $-\nabla^2\rho$ (au)

	ρ	$\nabla^2\rho$	r[a]	ψ[b]
		H_2O		
O	0.942	−5.084	0.646	114.2
		H_2S		
S	0.195	−0.577	1.301	111.4
		H_2CO		
O	0.967	−5.546	0.642	107.7
		H_2CS		
S	0.200	−0.610	1.297	107.2
		$H_2O\cdots HF$		
O LP_1[c]	0.925	−4.865	0.651	114.8
O LP_2	0.947	−5.101	0.646	115.2
		$H_2S\cdots HF$		
S LP_1	0.196	−0.587	1.304	111.9
S LP_2	0.195	−0.574	1.300	114.2
		$H_2CO\cdots HF$		
O LP_1	0.950	−5.375	0.646	107.5
O LP_2	0.972	−5.591	0.641	109.4
		$H_2CS\cdots HF$		
S LP_1	0.202	−0.622	1.300	105.5
S LP_2	0.198	−0.590	1.297	110.3

[a] r is the distance of the critical point from the nucleus. [b] ψ is as defined in Figure 1 (with HF replaced by the LP). [c] LP_1 is *syn* to the hydrogen bond; LP_2 is *anti*.

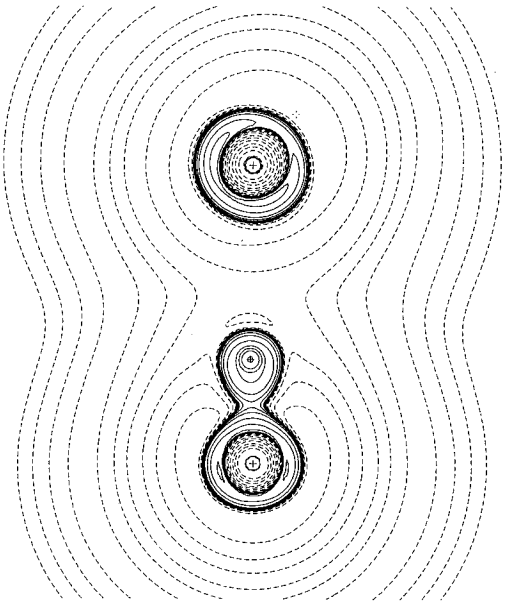

Figure 4. MP2/6-311++G(d,p) $-\nabla^2\rho$ distribution for $H_2O\cdots HF$ in the plane O···H−F.

The analyses of $-\nabla^2\rho$ found all the expected (3, −3) CPs in the valence shells of the monomers and complexes, and the LP results are summarized in Table 5. The $-\nabla^2\rho$ distributions in the complexes are also illustrated in Figures 4−7. The results for the monomers indicate that the oxygen bases are relatively "hard", with a large charge concentration held close to the O nucleus. The sulfur bases have more diffuse LPs located further

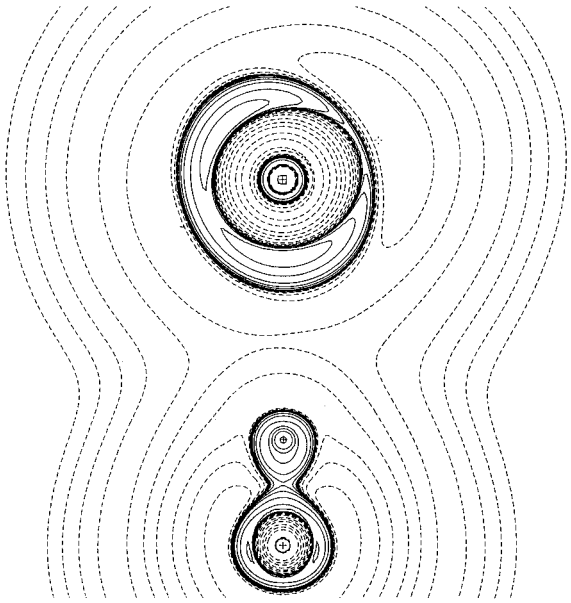

Figure 5. MP2/6-311++G(d,p) $-\nabla^2\rho$ distribution for $H_2S\cdots HF$ in the plane S···H−F.

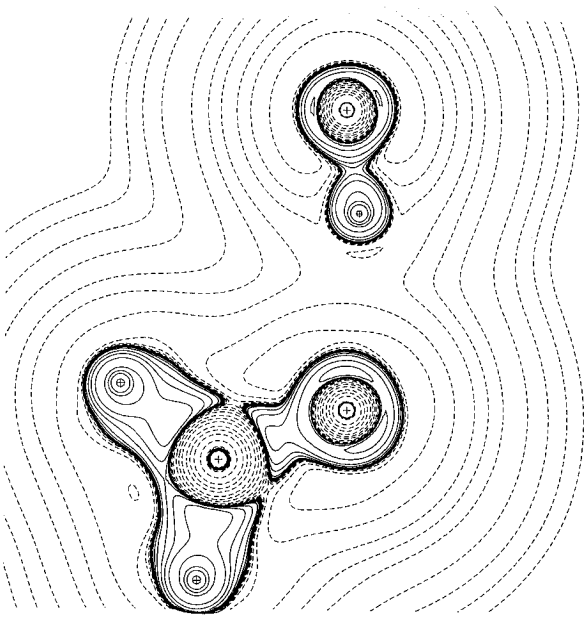

Figure 6. MP2/6-311++G(d,p) $-\nabla^2\rho$ distribution for $H_2CO\cdots HF$ in the plane O···H−F.

from the nucleus. In both H_2S and H_2CS the LP region does not have the largest concentration of density (one of the C···S bonded pairs has a more negative $\nabla^2\rho$ value), suggesting that an acid such as HF need not bond to the LP region in the manner indicated in Figure 1. That such a H bond *is* found in practice is apparently due to the LP density being more available for H bonding (in a steric sense) than the density found in the C−S and H−S covalent bonds.

The preferred approach of HF corresponds only very approximately to the position of the LP (3, −3) CP in $-\nabla^2\rho$ in the four bases (compare the column headed ψ in Table 5 with the ψ values in Table 1b, and see also Figures 4−7). The differences in LP angular position between the analogous sulfur and oxygen bases (2.8° and 0.5°, respectively) are very small compared to the variations in hydrogen-bonding angle observed (27.6° and 24.2°) for H_2Y and H_2CY, respectively. That $\nabla^2\rho$ fails to recover this geometrical detail is perhaps surprising in light of the conclusions of Carroll and Bader's initial study.[3]

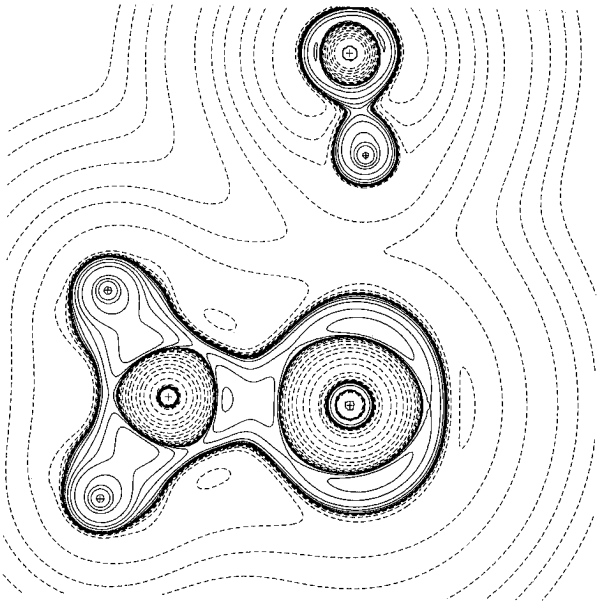

Figure 7. MP2/6-311++G(d,p) $-\nabla^2\rho$ distribution for $H_2CS\cdots HF$ in the plane S···H−F.

However, Wiberg *et al.*[25] also found differences of up to 20° between LP and hydrogen-bonding angles for a series of oxygen-containing bases. The small differences in LP angular position for oxygen and sulfur compounds suggest that the orbital hybridization is in fact very similar, and cannot be invoked as the origin of sulfur's perpendicular H bonding. The large differences between the angular position of the LP and the H-bonding angles found in practice also suggest that the use of the H bond direction as an alternative probe of LP direction[25,26] is dubious.

The LP values of $\nabla^2\rho_c$ change little on H bond formation, typically by around 2% in the oxygen complexes and rather less than 1% in the sulfur complexes. Oxygen LPs *syn* to HF are typically depleted, while on S these are enhanced. There is no evidence of any twisting of the LPs to align with the acid; the angles to the LPs hardly change on hydrogen bonding, and if anything, the *anti* LPs' positions change more than those of the *syn* LPs. The small size of all these changes is in harmony with the established fact that an electrostatic treatment of the hydrogen bond usually works well.

III. Atomic Properties. Integrated atomic populations and energies, including a breakdown of the atomic potential energies, can be found in Table 6. Changes in these properties on hydrogen bonding reflect the forces driving the formation of the hydrogen bond. One easily-visualized change is the extent of charge transfer from base to acid. For H_2O and H_2CO 0.035 and 0.037 electron is transferred, respectively. This electron density is accepted solely by the F of H−F: the hydrogen actually loses charge on hydrogen bond formation. Though the transferred density must pass through the shared interatomic surface of O and H_a (so that strictly speaking charge is transferred from O to H_a), the donating oxygen in both complexes actually increases its population, and in H_2CO the carbon also gains charge. So the hydrogens of the base are the source of the density which is ultimately transferred to HF. This effect, of hydrogen atoms acting as "reservoirs" of charge density to be donated on chemical interaction, has also been recognized in theoretical studies on protonation,[27] and it is noteworthy that it also holds for the much weaker and chemically distinct process of H bond formation.

(25) Wiberg, K. B.; Marquez, M.; Castejon, H. *J. Org. Chem.* **1994**, *106*, 1594.

(26) Chalasinski, G.; Szczéniak, M. M. *Chem. Rev.* **1994**, *94*, 1723.

Table 6. Atomic Populations and Energies in Complexes, and Changes[a] on H Bond Formation (au)[b]

	O or S	C	H_1[c]	H_2	H_a	F
			$H_2O\cdots HF$			
N	9.155 (+0.022)		0.405 (−0.029)	0.405 (−0.029)	0.270 (−0.019)	9.766 (+0.054)
E	−75.565 (−0.048)		−0.361 (+0.018)	−0.361 (+0.018)	−0.281 (+0.015)	−100.001 (−0.018)
V_{NE}[d]	−213.580 (−19.352)		−2.914 (−0.513)	−2.914 (−0.513)	−2.467 (−0.744)	−267.869 (−19.078)
V_{NEO}	−184.468 (−0.038)		−0.680 (+0.034)	−0.680 (+0.034)	−0.500 (+0.029)	−243.503 (−0.2851)
V_{REP}	+62.429 (+19.231)		+2.191 (+0.549)	+2.191 (+0.549)	+1.900 (+0.759)	+64.842 (+19.010)
			$H_2S\cdots HF$			
N	15.850 (+0.029)		1.053 (−0.037)	1.053 (−0.037)	0.296 (+0.008)	9.749 (+0.037)
E	−397.671 (−0.010)		−0.620 (+0.018)	−0.620 (+0.018)	−0.290 (+0.005)	−99.933 (+0.050)
V_{NE}	−986.618 (−27.046)		−9.447 (−1.197)	−9.447 (−1.197)	−3.022 (−1.299)	−277.114 (−28.323)
V_{NEO}	−947.453 (−0.4947)		−1.263 (+0.031)	−1.263 (+0.031)	−0.527 (+0.003)	−243.307 (−0.089)
V_{REP}	+191.276 (+27.282)		+8.207 (+1.232)	+8.207 (+1.232)	+2.441 (+1.301)	+77.284 (+28.452)
			$H_2CO\cdots HF$			
N	9.051 (+0.009)	5.013 (+0.016)	0.947 (−0.033)	0.952 (−0.029)	0.276 (−0.012)	9.761 (+0.049)
E	−75.719 (−0.014)	−37.314 (−0.009)	−0.603 (+0.013)	−0.606 (+0.010)	−0.285 (+0.011)	−100.006 (−0.023)
V_{NE}	−231.622 (−18.828)	−114.415 (−8.189)	−7.465 (−1.441)	−7.030 (−1.006)	−2.844 (−1.121)	−276.744 (−27.953)
V_{NEO}	−184.228 (−0.128)	−85.728 (−0.065)	−1.230 (+0.026)	−1.234 (+0.022)	−0.508 (+0.022)	−243.466 (−0.248)
V_{REP}	+80.183 (+18.797)	+39.786 (+8.169)	+6.257 (+1.466)	+5.817 (+1.026)	+2.274 (+1.133)	+76.736 (+27.904)
			$H_2CS\cdots HF$			
N	15.552 (−0.010)	6.544 (−0.004)	0.918 (−0.027)	0.928 (−0.017)	0.304 (+0.015)	9.755 (+0.043)
E	−397.514 (−0.064)	−38.178 (−0.009)	−0.588 (+0.011)	−0.593 (+0.007)	−0.293 (−0.003)	−99.940 (+0.044)
V_{NE}	−1007.839 (−27.546)	−142.886 (−10.243)	−8.649 (−1.451)	−8.164 (−0.966)	−3.486 (−1.763)	−287.093 (−38.302)
V_{NEO}	−944.478 (−0.171)	−91.296 (−0.010)	−1.202 (+0.023)	−1.210 (+0.014)	−0.532 (−0.002)	−243.337 (−0.155)
V_{REP}	+212.813 (+27.425)	+66.530 (+10.225)	+7.473 (+1.473)	+6.978 (+0.975)	+2.900 (+1.760)	+87.214 (+38.382)

[a] Values in parentheses are changes from monomer values. [b] 1 au of energy = 2625.5 kJ·mol^{-1}. [c] For compounds of the type H_2CY, H_1 is *syn* to H−F and H_2 is *anti* to H−F. [d] See the text for definitions of V_{NE} and V_{NEO}.

The pattern of changes in atomic populations can be viewed in two ways: as an overall flow of density from the slightly electropositive H_1 and H_2 through the complex to the electronegative fluorine or as charge transfer from O to H_a accompanied by charge rearrangement within each fragment to give the lowest overall energy. The sulfur-containing complexes show broadly similar behavior, but with some interesting differences. In both cases, H_a gains charge as well as F, presumably a result of the lesser electronegativity of sulfur as opposed to oxygen, resulting in charge transfer of 0.045 and 0.058 electron from H_2S and H_2CS, respectively. H_2S changes in a very similar fashion to H_2O, with S gaining charge at the expense of its own hydrogens. However, in H_2CS the electron population falls in both sulfur and carbon, and in the attached hydrogens. Overall, a significant difference between oxygen and sulfur complexes is that the sulfur bases may have donated more charge to the incoming acid, despite the fact that the sulfur atom itself carries a positive charge.

Atomic energies reveal where in the complex the stabilization due to hydrogen bonding occurs. Again it proves informative to sum atomic energy changes into fragment values; this summation highlights some major differences between the oxygen and sulfur complexes. Both $H_2O\cdots HF$ and $H_2CO\cdots HF$ undergo stablization in the acid *and* the base fragment: H_2O is stabilized by 33.1 kJ·mol^{-1}, while H_2CO is stabilized by just 1.1 kJ·mol^{-1}; *i.e.,* formation of $H_2O\cdots HF$ is driven by stabilization of the base, but formation of $H_2CO\cdots HF$ is due to stabilization of the acid. The sulfur complexes behave quite differently, with very large stabilizations in the base fragment (169.1 and 143.1 kJ·mol^{-1} for H_2S and H_2CS) offset by large destabilizations of the acid. At the atomic level, the oxygen complexes show stabilization of oxygen (and carbon in H_2CO) on H bond formation balanced by destabilization of the hydrogens. Both complexes have fluorine stabilized and H_a destabilized. A similar picture emerges for the sulfur compounds, where the large base stabilizations noted above are concentrated almost entirely in the sulfur basins, with a small stabilization of C in H_2CS. Unlike in the oxygen-containing complexes, both fluorine and H_a are destabilized, despite accepting charge density from the base. A full understanding of these changes requires a decomposition of the potential energy into its components V_{NE}, V_{NEO}, and V_{REP}.

The approach of two molecules from infinite separation inevitably leads to an increase in each molecule's attractive (V_{NE}) and repulsive (V_{REP}) potential energies. This is evident in the atomic changes in these potential energies (Table 6), which show changes of up to 38 hartrees (1 hartree = 2625.5 kJ·mol^{-1}). The overall atomic energy changes are several orders of magnitude smaller than these potential energy changes, so the interplay between them must be finely balanced. It is helpful to further partition the change in attractive potential energy into two terms, ΔV_{NEO} and $\Delta(V_{NE} - V_{NEO})$, which refer to changes in *intraatomic* and *interatomic potential energy*, respectively. (Here intraatomic means the attractive potential energy between a nucleus and the electrons within its *own* atomic basin; interatomic stabilization of an atom is the contibution to V_{NE} from its electrons and the nuclei of *other* atoms.)

H bond formation leads to interatomic stabilization in every atom in all four complexes. Generally, those atoms in which the *total* energy is lowered on H bond formation also undergo intraatomic stabilization. This trend has been noted before for hydrogen-bonded systems,[6] and suggests that intraatomic effects play an important role in tipping the balance between attractive and repulsive forces, depsite the much larger changes in interatomic energies. The only atoms which do not follow this trend are the fluorines in the sulfur complexes. For these atoms, the increase in repulsive energy on complexation dominates the total energy change, and they are destabilized despite having increased intra- and interatomic stabilization. This accounts for the unusual relationship between population and energy changes in these fluorines (atoms gaining electrons are usually stabilized): they are electronegative in that they are able to stabilize density within their basins, and therefore withdraw density from their surroundings. In the act of H bond formation they are

(27) (a) Stutchbury, N. C. J.; Cooper, D. L. *J. Chem. Phys.* **1983**, *79*, 4967. (b) Howard, S. T.; Platts, J. A. *J. Chem. Phys.* **1995**, *99*, 9027.

Table 7. Selected Multipole Moments on the Base Atom O or S (au)

	H_2O	H_2S	H_2CO	H_2CS
q	−1.133	+0.180	−1.041	+0.438
M_Z[a]	+0.177	−0.908	+0.434	−1.276
Q_{XX}	+1.312	+4.505	+0.022	−0.213
Q_{YY}	−1.425	−6.873	−0.581	−6.058
Q_{ZZ}	+0.113	+2.368	+0.559	+6.271

[a] See Figure 1 for the axis system employed.

drawn closer toward the sulfur atom, and the resulting repulsion between the electron density in the fluorine and sulfur basins outweighs the increase in the intra- and interatomic stabilizations. Since this situation is only found for the sulfur complexes, it suggests that sulfur's eight extra core electrons may be the source of the excess repulsion.

Table 7 contains atomic charges, dipoles, and quadrupoles for the oxygen or sulfur atom in the monomers (a list of all multipole moments has been deposited as supporting information). An obvious feature is the difference in atomic charge on oxygen and sulfur. Similarly, the atomic dipoles on O and S differ in sign; that on oxygen reflects a polarization of density toward the positive C and/or H atoms, but in the sulfur-containing molecules, these atoms are negative and the sulfur dipole has its positive lobe in the LP region. The atomic quadrupoles on O and S, on the other hand, have the same sign in all cases, the negative *yy* quadrupole reflecting the lone-pair structure present in all four molecules. An important result is the much greater magnitudes of the dipole and quadrupole polarizations on S compared to O, up to 10 times larger for some quadrupoles. This has an important effect on the electrostatic properties discussed below.

Changes in the atomic dipole moments on complex formation are generally small: ∼0.1 au for oxygen or sulfur in the $H_2Y\cdots HF$ complexes, and ∼0.01 au in the $H_2CY\cdots HF$ complexes. These changes can be linked to the changes in atomic population discussed above, since the values are determined by the atomic charges to a large extent.[28] The charge flow from base to acid results in larger positive charges on the hydrogens in the O complexes and smaller negative charges in the S complexes. Thus, in the former the O dipole is enhanced and in the latter the S dipole is reduced. The quadrupole moments of sulfur and oxygen show larger changes, typically ∼0.4 au, retaining their sign from the free bases but diminishing in magnitude. The reduction of these moments in the complex probably reflects the presence of the new interatomic surface between the base atom and H_a (*i.e.*, the atomic basin no longer extends to infinity in this direction) rather than any loss of density from the LP due to H bond formation.

IV. Electrostatics. The monomer multipole moments may be used to expand both the MEP and the electrostatic intermolecular stabilization, and therefore to predict the H-bonding geometry using electrostatics *a la* Buckingham and Fowler. This expansion is exact only if all multipole moments are employed; our treatment truncates it at the quadrupole level, with associated series termination errors. To see if these are acceptably small, we compared the MEP from this expansion with that calculated directly from the MP2 wave function. Even at the site which would be occupied by the H atom of HF in the complex, the base MEP is well-represented by a many-center multipole expansion up to quadrupole level with the AIMs moments (a table of the exact vs multipole expanded potential is included in the supporting information). The worst discrepancy at this distance is for H_2S (17%). The agreement improves with distance from the basic atom, until the values are essentially identical at 1.5 Å beyond the H bond distance.

(28) (a) Laidig, K. E.; Bader, R. F. W. *J. Chem. Phys.* **1990**, *93*, 7213. (b) Howard, S. T. *Mol. Phys.* **1995**, *85*, 395.

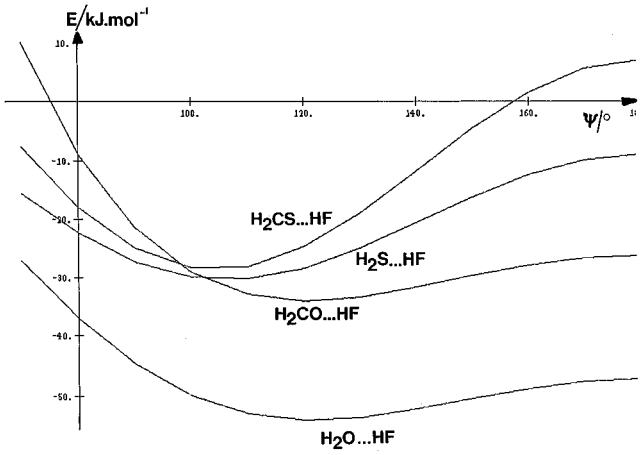

Figure 8. Electrostatic energy versus H bond orientation ψ for the four complexes.

Intermolecular electrostatic interaction energies are obtained by the pairwise summation of multipole−multipole interactions between all pairs of atoms in separate molecules. Table 8 contains the values of ψ at which these energies are minimized, along with the interaction energy and its components at this geometry (Figure 8 shows their variation with ψ). The agreement of these electrostatic predictions with the calculated results in Tables 1 and 2 is semiquantitative. The electrostatic model recovers the two major differences between the oxygen and sulfur complexes; *i.e.*, (i) the sulfur complexes are predicted to be more weakly bound, and (ii) the optimum ψ is ∼16° less than in the oxygen complexes. The predicted geometries are rather better than those employing the maxima in $-\nabla^2\rho$, confirming that AIMs multipole moments are suitable for this type of treatment. The discrepancies between the exact and electrostatic model energies may be accounted for by charge-transfer and inductive/dispersive contributions to the H bond energy, although the general success of the Buckingham−Fowler model suggests these are usually small. These researchers have also obtained better accuracy in predicting H-bonding geometries and energies in a number of complexes, probably because their models were fully geometry-optimized (we have not optimized θ in our electrostatic estimates).

Whatever the reason for these differences, the primary aim here is not to make the most accurate possible predictions of these properties, but to explain the observed trends. The multipole expansion of the interaction energy can identify those terms which drive the H bond formation, and which determine the optimum ψ. From Table 8 it is clear that a H bond to oxygen is dominated by the charge−charge term (in particular the interaction of O and H_a). The repulsive charge−dipole term is large, but not so large as to offset the charge−charge attraction. By contrast, the positive charge on sulfur leads to a repulsive charge−charge term in these complexes. H bond formation in this case is driven by charge−dipole and charge−quadrupole interactions, since the dipoles and quadrupoles are much larger on S than on O. Changes in the contributions to E_{tot} with varying ψ reveal which interactions prefer a linear arrangement ($\psi = 180°$), and which tend to pull H−F into a more perpendicular orientation. For the oxygen complexes only two terms, E_{md} and E_{mq}, prefer the perpendicular orientation, whereas three, E_{mm}, E_{mq}, and E_{dd}, act to make the sulfur complexes more perpendicular. Crucially, one of these (E_{mq}) plays a major role in H bond formation.

Table 8. Predicted Geometries and Energies[a] from the Electrostatic Energy (deg and kJ·mol^{-1})

	optimum ψ	E_{tot}	E_{mm}	E_{md}	E_{mq}	E_{dd}	E_{dq}	E_{qq}	$E_{complex}$
$H_2O\cdots HF$	121.5	−54.07	−84.70	+50.96	−19.64	−7.59	+6.54	+0.13	−73.87
$H_2S\cdots HF$	106.0	−30.24	+7.82	−12.71	−42.77	+3.33	+13.94	+0.11	−44.21
$H_2CO\cdots HF$	120.5	−34.02	−103.60	+86.67	+0.26	−17.28	−0.04	−0.03	−61.93
$H_2CS\cdots HF$	104.5	−28.54	+24.94	−34.87	−40.70	+8.77	+13.15	+0.18	−29.67

[a] E_{tot} is the total interaction energy, E_{mm} is the charge−charge term, E_{md} is the monopole−dipole term, E_{mq} the monopole−quadrupole term, *etc*.

Conclusions

The key differences between H-bonded complexes of oxygen and sulfur compounds have been identified from calculations on their complexes with HF. A sulfur base is more weakly bound than its oxygen analogue, and prefers a much more perpendicular orientation of HF relative to the basic atom. This result is supported by a database search of suitable intermolecular contacts in molecular crystals. These differences have their origin in the multipole moments of the base atom; notably the monopole and dipole of oxygen and sulfur differ in both sign and magnitude. A multipolar electrostatic treatment of these H bonds reveals that the O···H interaction is dominated by charge−charge attraction, while S···H is stabilized mainly by the charge (H)−quadrupole (S) interaction. The driving force in forming H bonds to oxygen, the monopole−monopole term, prefers a linear orientation, while the monopole−dipole and monopole−quadrupole terms driving H bond formation to sulfur prefer $\psi = 90°$. The Laplacian of the charge density does not predict these observed differences in directionality.

Although the direction and binding energy of the H bonds are reasonably well-represented by an electrostatic model, an atoms-in-molecules analysis of the internal changes in energy of the basic and acidic fragments reveals fundamentally different behavior in oxygen and sulfur compounds. The former show stabilization in both the base *and* the acid moieties, whereas only the acid is destabilized in sulfur complexes. All complexes show a small charge transfer from base to acid (larger in the sulfur complexes), with this charge flowing ultimately from the hydrogens on the base.

These results show that it is not necessary to invoke hybridization arguments to explain geometrical differences in sulfur and oxygen hydrogen bonds. In fact, the similarity in sulfur and oxygen of the LP orientation, as characterized by the $-\nabla^2\rho$ topology, suggests there is little qualitative difference between these atoms in their divalent R−Y−R and $R_2C{=}Y$ compounds.

Acknowledgment. We thank the U.K. Engineering and Physical Sciences Research Council for a Ph.D. Studentship (J.A.P.), an Advanced Fellowship (S.T.H.), and a Post-Doctoral Research Assistantship (B.R.F.B.).

Supporting Information Available: Tables giving monomer and complex atomic multipole moments and exact and multipole electrostatic potentials (3 pages). This material is contained in many libraries on microfiche, immediately follows this article in the microfilm version of the journal, can be ordered from the ACS, and can be downloaded from the Internet; see any current masthead page for ordering information and Internet access instructions.

JA952871S